Atmospheric Chemistry and Physics Discussions

Radical loss in the atmosphere from Cu-Fe redox coupling in aerosols

J. Mao[1,2], S. Fan[2], D. J. Jacob[3], and K. R. Travis[3]

[1]Program in Atmospheric and Oceanic Sciences, Princeton University, Princeton, NJ 08542, USA
[2]Geophysical Fluid Dynamics Laboratory/National Oceanic and Atmospheric Administration, Princeton, NJ 08542, USA
[3]School of Engineering and Applied Sciences, Harvard University, Cambridge, MA 02138, USA

Correspondence to: J. Mao (jingqiu.mao@noaa.gov)

27053

Abstract

The hydroperoxyl radical (HO_2) is a major precursor of OH and tropospheric ozone. OH is the main atmospheric oxidant, while tropospheric ozone is an important surface pollutant and greenhouse gas. Standard gas-phase models for atmospheric chemistry tend to overestimate observed HO_2 concentrations, and this has been tentatively attributed to heterogeneous uptake by aerosol particles. It is generally assumed that HO_2 uptake by aerosol involve conversion to H_2O_2, but this is of limited efficacy as an HO_2 sink because H_2O_2 can photolyze to regenerate OH and from there HO_2. Joint atmospheric observations of HO_2 and H_2O_2 suggest that HO_2 uptake by aerosols may in fact not produce H_2O_2. Here we propose a catalytic mechanism involving coupling of the transition metal ions (TMI) Cu(I)/Cu(II) and Fe(II)/Fe(III) to rapidly convert HO_2 to H_2O in aerosols. The implied HO_2 uptake significantly affects global model predictions of tropospheric OH, ozone, and other species, improving comparisons to observations, and may have a major and previously unrecognized impact on atmospheric oxidant chemistry.

1 Introduction

HO_2 in the troposphere cycles rapidly with other members of the hydrogen oxide radical family ($HO_x \equiv OH + H + HO_2 +$ organic peroxy and oxy radicals). This cycling determines OH levels and ozone production. The main sources of HO_x are photolysis of ozone in the presence of water vapor and photolysis of carbonyls. The sinks involve formation of peroxides, HNO_3, and water. Peroxides and HNO_3 can photolyze, returning HO_x. Formation of water is a terminal sink. HO_2 is in general the dominant component of HO_x, so that the budget of HO_2 is largely defined by that of HO_x.

Uptake of HO_2 by aqueous aerosols is promoted by its high solubility in water (Henry's law constant $2.0 \times 10^3 \, M \, atm^{-1}$ at 298 K) and aqueous-phase dissociation to O_2^- ($pK_a = 4.7$), with rapid ensuing ionic redox chemistry. The efficacy of uptake is com-

27054

monly measured by the reactive uptake coefficient, $\gamma(HO_2)$, defined as the fraction of HO_2 collisions with aerosol surfaces resulting in reaction. Direct reaction of $HO_2(aq)$ with O_2^- produces H_2O_2 but the corresponding $\gamma(HO_2)$ is relatively low, ranging from 0.01 for acidic aerosols (Thornton and Abbatt, 2005) to 0.2 for neutralized aerosols (Thornton and Abbatt, 2005; Taketani et al., 2008). Higher values of $\gamma(HO_2)$, approaching unity, have been measured for Cu-doped aerosols where Cu(I)/Cu(II) redox cycling catalyzes HO_2^-/O_2^- conversion to H_2O_2 (Mozurkewich et al., 1987; Cooper and Abbatt, 1996; Thornton and Abbatt, 2005; Taketani et al., 2008). Model calculations suggest that other aerosol TMI, including Fe(II)/Fe(III) and Mn(II)/Mn(III), can drive similar chemistry (Graedel et al., 1986). Uptake of HO_2 by non-aqueous inorganic aerosol appears to be very slow (Cooper and Abbatt, 1996; Taketani et al., 2008), but can be significant for organic aerosols (up to 0.13 for levoglucosan particles) (Taketani et al., 2010).

Standard gas-phase models for atmospheric chemistry tend to overestimate observed HO_2 concentrations, and this has been tentatively attributed to heterogeneous uptake by aerosol particles. As shown in Table 1, HO_x loss by HO_2 uptake is only significant where the gas-phase photochemistry controlling HO_x levels is slow (HO_2 is typically less than 10 ppt) and/or aerosol loading is high. To a large extent this is because HO_x loss through $HO_2 + HO_2$ and $HO_2 + RO_2$ is quadratic on HO_x concentrations.

All the laboratory and model mechanisms for HO_2 uptake by aerosol involve conversion to H_2O_2 (Mozurkewich et al., 1987; Hanson et al., 1992; Gershenzon et al., 1995; Cooper and Abbatt, 1996; Remorov et al., 2002; Thornton and Abbatt, 2005; Taketani et al., 2008, 2009; Thornton et al., 2008; Loukhovitskaya et al., 2009; Macintyre and Evans, 2011), but this is of limited efficacy as an HO_2 sink because H_2O_2 can photolyze to regenerate OH and from there HO_2. Joint atmospheric observations of HO_2 and H_2O_2 suggest that HO_2 uptake by aerosols may in fact not produce H_2O_2 (de Reus et al., 2005; Mao et al., 2010). Previous proposed mechanisms for the conversion of HO_2 to H_2O, including $Br_2^- + HO_2$ (Matthew et al., 2003), $HSO_4^- + HO_2$ (Cooper and Abbatt, 1996), and the HO_2–H_2SO_4 complex (Miller and Francisco, 2001) are not catalytic and thereby less efficient. Here we propose a catalytic mechanism involving coupling

of the transition metal ions (TMI) Cu(I)/Cu(II) and Fe(II)/Fe(III) to rapidly convert HO_2 to H_2O in aerosols (Fig. 1).

2 Cu-Fe-HO_x cycling

Cu and Fe are ubiquitous components of crustal and combustion aerosols. Concentrations in rural air are in the range 3–300 $ng\,m^{-3}$ for Cu and 55–14 500 $ng\,m^{-3}$ for Fe (Schroeder et al., 1987). The submicron size fraction generally associated with combustion aerosols accounts for 25–100 % of Cu mass and 15–50 % of Fe mass (Tables S1 and S2). Joint measurements of Cu and Fe in fine particles ($PM_{2.5}$) show that Cu/Fe ratio is typically below 0.1 (Table S3; Fig. S3). While Cu tends to fully dissolve at pH < 5 (Deguillaume et al., 2005), the solubility of Fe varies greatly, ranging from less than 1 % in soils to 81 % in oil combustion products (Schroth et al., 2009). Observations indicate that the dissolved Cu to Fe molar ratio (hereinafter "Cu/Fe") is typically 0.01–0.1 (Table S4).

Cu-catalyzed HO_2 loss to H_2O_2 in acid aerosols proceeds by Reactions (RA1) and (RA2), with similar reactions involving O_2^- for higher-pH conditions:

$$Cu(II) + HO_2 \rightarrow Cu(I) + O_2 + H^+ \tag{RA1}$$

$$Cu(I) + HO_2 \xrightarrow{H^+} Cu(II) + H_2O_2 \tag{RA2}$$

$$Cu(I) + O_2 \xrightarrow{H^+} Cu(II) + HO_2 \tag{RA3}$$

Here the destruction of HO_2 is buffered by the internal production of HO_2 via Reaction (RA3) (Ervens et al., 2003). Fe-catalyzed HO_2 loss proceeds by a similar cycle though the rate constant of Fe(III) + HO_2 is two orders of magnitude slower than for Cu(II) (Mozurkewich et al., 1987).

The coupled Cu-Fe catalytic cycle for aqueous-phase HO_2 loss involves Reaction (RA1) and

$$Cu(I) + Fe(III) \rightarrow Cu(II) + Fe(II) \quad\quad (RA4)$$

with three likely pathways for Fe(II) to close the cycle:

$$Fe(II) + HO_2 \xrightarrow{H^+} Fe(III) + H_2O_2 \quad\quad (RA5)$$

$$Net: HO_2 + HO_2 \rightarrow H_2O_2 + O_2$$

$$Fe(II) + H_2O_2 \rightarrow Fe(III) + OH + OH^- \quad\quad (RA6)$$

$$Net: HO_2 + H_2O_2 \rightarrow OH + O_2 + H_2O$$

$$Fe(II) + OH \rightarrow Fe(III) + OH^- \quad\quad (RA7)$$

$$Net: HO_2 + OH \rightarrow O_2 + H_2O$$

The electron transfer reaction Cu(I) + Fe(III) (RA4) is rapid with a rate constant of $1.3\text{–}3 \times 10^7\,M^{-1}\,s^{-1}$ (Bjergbakke et al., 1976; Sedlak and Hoigné, 1993). It has been found previously to regulate the observed diurnal pattern of the Fe(II)/Fe(III) ratio in cloud water (Ervens et al., 2003; Deguillaume et al., 2004). Aerosol chemistry models suggest that Reaction (RA1) is the dominant sink for Cu(II) (Jacob et al., 1989), and we show below that Reaction (RA4) is then the dominant sink for Cu(I) over the expected range of Cu/Fe ratios. The implications for HO_x depend on the fate of Fe(II). Reaction (RA5) converts HO_x to H_2O_2 while Reaction (RA7) converts HO_x to H_2O Reaction (RA6) also effectively leads to HO_x loss by converting H_2O_2 to H_2O.

3 Formulation of HO_2 reactive uptake by aerosols

We conducted box model simulations of aqueous aerosol chemistry to examine the effect of Cu-Fe-HO_x cycling by Reactions (RA1)–(RA7) on the HO_x chemical budget. The

chemical mechanism mainly draws from Jacob (2000) and Deguillaume et al. (2004), with a number of modifications and updates (Tables S8 and S9). A few complexes are included to take into account the speciation of Fe and Cu: $Fe(OH)^+$, $Fe(OH)_2^+$, $Fe(SO_4)^+$, $Fe(OH)^{2+}$, and $CuSO_4(aq)$. Our simulations are for $T = 298\,K$ as kinetic data are often not available at low temperatures.

Modeling aerosol aqueous chemistry must account for ionic strength corrections. We use the aerosol inorganic model (Clegg et al., 1998), to calculate the ionic strength and activity coefficients for major ions (i.e. NH_4^+, H^+, HSO_4^-, SO_4^{2-}) (Table S6). Activity coefficients for trace metal ions and neutral species are calculated based on specific ion interaction theory or estimated following Ross and Noone (1991) (Supplement, summarized in Table S7). We also account for the salting out effect on Henry's law constants. We assume Henry's law equilibrium for H_2O_2, O_3, and O_2 because of their long lifetimes. Gas uptake of OH is negligible compared to its aqueous production so that OH(aq) is calculated from aqueous-phase steady state. Concentrations of total dissolved Cu and Fe are held fixed throughout the simulation at their initial values.

The HO_2 uptake and volatilization rates R_{in} and R_{out} (molecules $cm^{-3}\,s^{-1}$) for a monodisperse aqueous aerosol of radius a can be approximated as (Jacob, 2000):

$$R_{in} = \left(\frac{a}{D_g} + \frac{4}{v\alpha}\right)^{-1} An_{HO_2} \quad\quad (1)$$

and

$$R_{out} = \left(\frac{a}{D_g} + \frac{4}{v\alpha}\right)^{-1} A\frac{[HO_2]_{surf}}{H^*} \quad\quad (2)$$

where n_{HO_2} is the gas phase concentration of HO_2, A is the aerosol surface area per unit volume of air, v is the mean molecular speed, α is the mass accommodation coefficient assumed to be unity (Thornton and Abbatt, 2005), D_g is the HO_2 gas phase

diffusion constant ($0.25\,\mathrm{cm^2\,s^{-1}}$), $[HO_2]_{surf}$ is the concentration at the aerosol surface, and H^* is the Henry's law constant corrected by ionic strength.

The chemical loss rate of aqueous HO_2 is the difference between R_{in} and R_{out}. $\gamma(HO_2)$ is then defined as the ratio of chemical loss rate to R_{in}. Given the short lifetime of aqueous HO_2 ($\sim 10^{-5}\,\mathrm{s}$) against reaction with Cu(II) by Reaction (RA1), the bulk concentration $[HO_2]_{bulk}$ and surface concentration $[HO_2]_{surf}$ may differ substantially. On the basis of the solution to a steady state diffusion equation, their relationship can be expressed as (Jacob, 1986):

$$[HO_2]_{surf} = \frac{P_{HO_2}}{k^l} + \left([HO_2]_{bulk} - \frac{P_{HO_2}}{k^l} \right) \cdot \left[3 \left(\frac{\coth q}{q} - \frac{1}{q^2} \right) \right]^{-1} \tag{3}$$

where k^l is the first-order loss constant of HO_2, P_{HO_2} is the aqueous-phase production rate of HO_2, and $q = a(\frac{k^l}{D_{aq}})^{\frac{1}{2}}$ is the diffuso-reactive parameter, in which D_{aq} is the HO_2 aqueous phase diffusion constant. P_{HO_2} is mainly from Reaction (RA3).

4 Atmospheric model simulations

Figure 2 shows the aqueous-phase chemical budgets of $O_2(-I) \equiv HO_2(aq) + O_2^-$, H_2O_2, Cu, and Fe for a $0.35\,\mu\mathrm{m}$ (dry radius) NH_4HSO_4 aerosol at RH = 85 %, with dissolved Cu of $2.9 \times 10^{-3}\,\mathrm{M}$ and Cu/Fe = 0.05 (molar). The concentration of Cu is estimated from the measured size distribution of Cu in rural aerosols with total Cu of $3.1\,\mathrm{ng\,m^{-3}}$ (Ross and Noone, 1991). Reactions responsible for less than 1 % of total production or loss are not shown. In particular, we find that Fe(III) + Cu(I) completely dominates over other pathways for Fe(III) reduction including photolysis and Fe(III) + HO_2.

In contrast to cloud chemistry (Jacob, 2000), the HO_x budget in aerosols is mainly controlled by TMI chemistry because TMI concentrations are so high. Aqueous OH production and loss are dominated by Reactions (RA6) and (RA7), respectively. Aque-

27059

ous HO_2 production within the aerosol accounts for less than 2 % of its loss as Reaction (RA4) dominates over Reaction (RA3). The major sinks of aqueous HO_2 are Reactions (RA1) and (RA5). As shown in Fig. 2, 70 % of HO_2 taken up from the gas phase is chemically lost, with the remainder volatilizing. Therefore $\gamma(HO_2)$ under these conditions is equal to 0.7.

The Cu/Fe ratio is a critical factor in this model calculation. When Cu/Fe > 1, Reactions (RA2) and (RA3) are the dominant sinks for Cu(I), leading to the conversion of HO_2 to H_2O_2. Aerosol pH is also critical. Acid-base dissociation of $HO_2(aq)/O_2^-$ at higher pH decreases the HO_2 volatilization flux as the reaction rate constants of Cu or Fe with O_2^- can be two orders of magnitude faster than with $HO_2(aq)$. The speciation of Cu and Fe is affected by pH, and we account for some of the complexation equilibria as described in Sect. 3. Precipitation of $Fe(OH)_3$ could take place at pH > 4, but we assume this to be negligible due to high ionic strength ($A(Fe^{3+}) = 0.01$) and slow kinetics.

Figure 3a shows the pH dependence of our calculated $\gamma(HO_2)$ for ammonium-sulfate aerosol at various Cu/Fe ratios. Aerosol pH is held fixed throughout each simulation. For a given Cu/Fe, $\gamma(HO_2)$ approaches unity with increasing pH, reflecting enhanced chemical loss of O_2^- and therefore reduced volatilization flux. This pH dependence of $\gamma(HO_2)$ is consistent with laboratory measurements. Mozurkewich et al. (1987) found higher $\gamma(HO_2)$ with neutral Cu-doped aerosols ($LiNO_3$) ($\gamma(HO_2) = 0.94$) than acidic Cu-doped aerosols (NH_4HSO_4) ($\gamma(HO_2) = 0.40$). At fixed pH, $\gamma(HO_2)$ increases with decreasing Cu/Fe ratio, resulting from the suppressed HO_2 production by Reaction (RA3) and enhanced HO_2 loss by Fe(III) + $O_2(-I)$.

The TMI chemistry initiated by HO_2 uptake from the gas phase can lead to either production or loss of H_2O_2 (Fig. 1), and this can be expressed as a positive or negative H_2O_2 yield ($Y_{H_2O_2}$) associated with $\gamma(HO_2)$. Figure 3b shows the pH dependence of over a range of Cu/Fe ratios. $Y_{H_2O_2} = 0.5$ indicates that all HO_2 is converted to H_2O_2, $Y_{H_2O_2} = 0$ indicates that all HO_2 is converted to H_2O, and $Y_{H_2O_2} < 0$ indicates a reactive uptake of H_2O_2. When Cu/Fe ≤ 0.05, $Y_{H_2O_2}$ decreases with increasing pH. This is in

27060

part due to the enhanced loss of aqueous HO_2 by Reaction (RA1) and Fe(III) + $O_2(-I)$, resulting in suppressed production of H_2O_2 by Reaction (RA5). On the other hand, at higher pH, the oxidation of Fe(II) is enhanced by $Fe(OH)^+ + H_2O_2$ which is five orders of magnitude faster than $Fe^{2+} + H_2O_2$. Reactions (RA6) and (RA7) then become the dominant sinks for Fe(II) and may lead to a reactive uptake of H_2O_2 ($Y_{H_2O_2} < 0$). The slight increase of at Cu/Fe = 0.1 while pH increases from 0 to 3 is mainly due to the enhanced H_2O_2 production by Reaction (RA2). This pathway becomes unimportant at lower Cu/Fe.

Figure 3c examines the sensitivity of $\gamma(HO_2)$ to a decrease of Cu concentrations from the 2.9×10^{-3} M assumed in the standard simulation, keeping a fixed Cu/Fe = 0.05. We find that the sensitivity is weak as long as Cu remains above 5×10^{-4} M. For example, at pH = 3, $\gamma(HO_2)$ only decreases from 0.85 to 0.61 with a five-fold decrease of Cu concentrations. This weak response is mainly because uptake of HO_2 is limited by diffusion in the aqueous phase, reflecting its very fast reaction with Cu(II). As Cu(II) concentrations drop to values sufficiently low for HO_2 to become well-mixed into the aerosol, $\gamma(HO_2)$ then decreases rapidly with decreasing Cu. This dependence of $\gamma(HO_2)$ on Cu concentrations also appears to be consistent with laboratory measurements (Mozurkewich et al., 1987).

5 Global implications for atmospheric oxidant chemistry

We examine the potential global implications of Cu-Fe-HO_x cycling by incorporating the corresponding HO_2 uptake in the GEOS-Chem global model of aerosol-oxidant chemistry (v9-01-01, http://www.geos-chem.org). Values in Fig. 3a indicate $\gamma(HO_2)$ in the range 0.4–1 depending on pH and the Cu/Fe ratio at 298 K; $\gamma(HO_2)$ is more likely to approach 1 at colder temperatures because of the higher solubility of HO_2 (Mao et al., 2010). At these high values of $\gamma(HO_2)$, HO_2 uptake can be limited by gas-phase diffusion with little residual dependence on $\gamma(HO_2)$ (Fig. S1). Thus we assume here $\gamma(HO_2) = 1$ as a reasonable upper limit, and we further assume $Y_{H_2O_2} = 0$ (Fig. 3b),

since observations suggest that the dissolved Cu/Fe ratio is usually below 0.1 (Table S4); in fact, it appears from Fig. 3b that $Y_{H_2O_2}$ is more likely to be negative than positive. Finally, we assume as an upper limit that this reactive uptake of HO_2 proceeds on all non-cloud aerosol surfaces in GEOS-Chem (Martin et al., 2003), i.e., that Cu and Fe are internally mixed and that all aerosol particles are aqueous. The GEOS-Chem simulation has been successfully evaluated against global observations of aerosol optical depth (van Donkelaar et al., 2010). There remain large uncertainties in the aerosol phase and mixing state, and so the calculations presented here should only be viewed as illustrative of the potential effect. Other mechanisms than the Cu-Fe-HO_x redox chemistry described here could also contribute to HO_2 conversion to H_2O in aqueous aerosols (Sect. 2 in the Supplement) and help explain the fast HO_2 loss ($\gamma(HO_2) \sim 1$) inferred from field studies (Table 1).

Figure 4 shows the difference of annual mean surface air concentrations of OH, HO_2, CO, and O_3 during 2005 as a result of this HO_2 uptake. The effects are largest in the extratropical Northern Hemisphere, where aerosol loading is high and the gas-phase photochemistry controlling HO_x levels is relatively slow. Surface OH and HO_2 concentrations decrease by 20–30 % and 40–60 %, respectively over that region; the decrease in OH is partly compensated by an increase in NO_x concentrations. The global mean (mass-weighted) tropospheric OH concentration in GEOS-Chem decreases by 12 % from 12.4×10^5 to 11.0×10^5 molecules cm^{-3}, improving agreement with observational constraints from methylchloroform data ($10.8 \pm 0.8 \times 10^5$ molecules cm^{-3}) (Prinn et al., 2005). The N/S interhemispheric OH ratio decreases from 1.09 to 1.02, in better agreement with the best estimate of 0.98 derived from methylchloroform observation (Krol and Lelieveld, 2003). The conversion of HO_2 to H_2O is critical for this effect. A sensitivity simulation with $\gamma(HO_2) = 1$ and $Y_{H_2O_2} = 0.5$ shows only a 3 % decrease in global mean OH concentration.

The decrease of OH concentrations drives an annual mean increase of model CO concentrations by 20–30 ppb in the extratropical Northern Hemisphere, with maximum effect in spring. As shown in Fig. 5, this fully corrects the long-standing seasonal

GEOS-Chem bias in simulating CO observations at remote surface sites in that part of the world (Alvarado et al., 2010; Fisher et al., 2010; Kopacz et al., 2010). A similar CO bias in the extratropical Northern Hemisphere is found in other global models (Shindell et al., 2006) and may be similarly corrected.

Surface ozone concentrations decrease in general by 3–5 ppb over North America and most regions in Eurasia. The largest decreases (up to 20 ppb) are in East Asia and help to correct model overestimates of surface ozone in that region (Wang et al., 2008). Comparison with surface ozone observations in the US from the Clean Air Status and Trends Network (CASTNet) shows a decrease of mean model bias from +7 to +3 ppb (Fig. S2).

HO_2 conversion to H_2O in aqueous aerosols thus improves model simulations in several aspects and could have a major and previously unrecognized impact on atmospheric oxidant chemistry. Anthropogenic aerosol concentrations are expected to decrease globally in the coming decades as a result of policies for improving air quality (Meinshausen et al., 2011). Our work suggests that this could have a detrimental effect on ozone air quality while causing OH to increase. From a climate forcing perspective, our work suggests that decreasing aerosol could drive an indirect positive forcing due to increasing tropospheric ozone and an indirect negative radiative forcing due to faster oxidation of methane and hydrofluorocarbons (HFCs). Better understanding of aqueous HO_2 chemistry in an atmospheric context is clearly needed. Measurements of Cu and Fe speciation in atmospheric aerosols would be of particular value.

Supplementary material related to this article is available online at: http://www.atmos-chem-phys-discuss.net/12/27053/2012/ acpd-12-27053-2012-supplement.pdf.

27063

References

Alvarado, M. J., Logan, J. A., Mao, J., Apel, E., Riemer, D., Blake, D., Cohen, R. C., Min, K. E., Perring, A. E., Browne, E. C., Wooldridge, P. J., Diskin, G. S., Sachse, G. W., Fuelberg, H., Sessions, W. R., Harrigan, D. L., Huey, G., Liao, J., Case-Hanks, A., Jimenez, J. L., Cubison, M. J., Vay, S. A., Weinheimer, A. J., Knapp, D. J., Montzka, D. D., Flocke, F. M., Pollack, I. B., Wennberg, P. O., Kurten, A., Crounse, J., Clair, J. M. S., Wisthaler, A., Mikoviny, T., Yantosca, R. M., Carouge, C. C., and Le Sager, P.: Nitrogen oxides and PAN in plumes from boreal fires during ARCTAS-B and their impact on ozone: an integrated analysis of aircraft and satellite observations, Atmos. Chem. Phys., 10, 9739–9760, doi:10.5194/acp-10-9739-2010, 2010.

Bjergbakke, E., Sehested, K., and Rasmussen, O. L.: The reaction mechanism and rate constants in the radiolysis of Fe^{2+}-Cu^{2+} solutions, Radiat. Res., 66, 433–442, 1976.

Cantrell, C. A., Shetter, R. E., Gilpin, T. M., and Calvert, J. G.: Peroxy radicals measured during Mauna Loa observatory photochemistry experiment 2: the data and first analysis, J. Geophys. Res.-Atmos., 101, 14643–14652, 1996.

Cantrell, C. A., Edwards, G. D., Stephens, S., Mauldin, R. L., Zondlo, M. A., Kosciuch, E., Eisele, F. L., Shetter, R. E., Lefer, B. L., Hall, S., Flocke, F., Weinheimer, A., Fried, A., Apel, E., Kondo, Y., Blake, D. R., Blake, N. J., Simpson, I. J., Bandy, A. R., Thornton, D. C., Heikes, B. G., Singh, H. B., Brune, W. H., Harder, H., Martinez, M., Jacob, D. J., Avery, M. A., Barrick, J. D., Sachse, G. W., Olson, J. R., Crawford, J. H., and Clarke, A. D.: Peroxy radical behavior during the Transport and Chemical Evolution over the Pacific (TRACE-P) campaign as measured aboard the NASA P-3B aircraft, J. Geophys. Res., 108, 8797, doi:10.1029/2003jd003674, 2003a.

Cantrell, C. A., Mauldin, L., Zondlo, M., Eisele, F., Kosciuch, E., Shetter, R., Lefer, B., Hall, S., Campos, T., Ridley, B., Walega, J., Fried, A., Wert, B., Flocke, F., Weinheimer, A., Hannigan, J., Coffey, M., Atlas, E., Stephens, S., Heikes, B., Snow, J., Blake, D., Blake, N., Katzenstein, A., Lopez, J., Browell, E. V., Dibb, J., Scheuer, E., Seid, G., and Talbot, R.: Steady state

27064

free radical budgets and ozone photochemistry during TOPSE, J. Geophys. Res.-Atmos., 108, 8361, doi:10.1029/2002jd002198, 2003b.

Clegg, S. L., Brimblecombe, P., and Wexler, A. S.: Thermodynamic model of the system H^+-NH_4^{4+}-SO_4^{2-}-NO_3^--H_2O at tropospheric temperatures, J. Phys. Chem. A, 102, 2137–2154, doi:10.1021/jp973042r, 1998.

Commane, R., Floquet, C. F. A., Ingham, T., Stone, D., Evans, M. J., and Heard, D. E.: Observations of OH and HO_2 radicals over West Africa, Atmos. Chem. Phys., 10, 8783–8801, doi:10.5194/acp-10-8783-2010, 2010.

Cooper, P. L. and Abbatt, J. P. D.: Heterogeneous interactions of OH and HO_2 radicals with surfaces characteristic of atmospheric particulate matter, J. Phys. Chem., 100, 2249–2254, 1996.

de Reus, M., Fischer, H., Sander, R., Gros, V., Kormann, R., Salisbury, G., Van Dingenen, R., Williams, J., Zöllner, M., and Lelieveld, J.: Observations and model calculations of trace gas scavenging in a dense Saharan dust plume during MINATROC, Atmos. Chem. Phys., 5, 1787–1803, doi:10.5194/acp-5-1787-2005, 2005.

Deguillaume, L., Leriche, M., Monod, A., and Chaumerliac, N.: The role of transition metal ions on HO_x radicals in clouds: a numerical evaluation of its impact on multiphase chemistry, Atmos. Chem. Phys., 4, 95–110, doi:10.5194/acp-4-95-2004, 2004.

Deguillaume, L., Leriche, M., Desboeufs, K., Mailhot, G., George, C., and Chaumerliac, N.: Transition metals in atmospheric liquid phases. Sources, reactivity, and sensitive parameters, ChemInform, 36, doi:10.1002/chin.200549218 2005.

Ervens, B., George, C., Williams, J. E., Buxton, G. V., Salmon, G. A., Bydder, M., Wilkinson, F., Dentener, F., Mirabel, P., Wolke, R., and Herrmann, H.: CAPRAM 2.4 (MODAC mechanism): an extended and condensed tropospheric aqueous phase mechanism and its application, J. Geophys. Res., 108, 4426, doi:10.1029/2002jd002202, 2003.

Fisher, J. A., Jacob, D. J., Purdy, M. T., Kopacz, M., Le Sager, P., Carouge, C., Holmes, C. D., Yantosca, R. M., Batchelor, R. L., Strong, K., Diskin, G. S., Fuelberg, H. E., Holloway, J. S., Hyer, E. J., McMillan, W. W., Warner, J., Streets, D. G., Zhang, Q., Wang, Y., and Wu, S.: Source attribution and interannual variability of Arctic pollution in spring constrained by aircraft (ARCTAS, ARCPAC) and satellite (AIRS) observations of carbon monoxide, Atmos. Chem. Phys., 10, 977–996, doi:10.5194/acp-10-977-2010, 2010.

Gershenzon, Y. M., Grigorieva, V. M., Ivanov, A. V., and Remorov, R. G.: O_3 and OH sensitivity to heterogeneous sinks of HO_x and CH_3O_2 on aerosol particles, Faraday Discuss., 100, 83–100, 1995.

Graedel, T. E., Mandich, M. L., and Weschler, C. J.: Kinetic-model studies of atmospheric droplet chemistry: 2. Homogeneous transition-metal chemistry in raindrops, J. Geophys. Res.-Atmos., 91, 5205–5221, 1986.

Haggerstone, A. L., Carpenter, L. J., Carslaw, N., and McFiggans, G.: Improved model predictions of HO_2 with gas to particle mass transfer rates calculated using aerosol number size distributions, J. Geophys. Res.-Atmos., 110, D04303, doi:10.1029/2004jd005282, 2005.

Hanson, D. R., Burkholder, J. B., Howard, C. J., and Ravishankara, A. R.: Measurement of OH and HO_2 radical uptake coefficients on water and sulfuric-acid surfaces, J. Phys. Chem., 96, 4979–4985, 1992.

Jacob, D. J.: Chemistry of OH in remote clouds and its role in the production of formic-acid and peroxymonosulfate, J. Geophys. Res.-Atmos., 91, 9807–9826, 1986.

Jacob, D. J.: Heterogeneous chemistry and tropospheric ozone, Atmos. Environ., 34, 2131–2159, 2000.

Jacob, D. J., Gottlieb, E. W., and Prather, M. J.: Chemistry of a polluted cloudy boundary layer, J. Geophys. Res., 94, 12975–13002, doi:10.1029/JD094iD10p12975, 1989.

Kanaya, Y., Sadanaga, Y., Matsumoto, J., Sharma, U. K., Hirokawa, J., Kajii, Y., and Akimoto, H.: Daytime HO_2 concentrations at Oki Island, Japan, in summer 1998: comparison between measurement and theory, J. Geophys. Res.-Atmos., 105, 24205–24222, 2000.

Kanaya, Y. G., Cao, R. Q., Kato, S. G., Miyakawa, Y. K., Kajii, Y., Tanimoto, H., Yokouchi, Y., Mochida, M., Kawamura, K., and Akimoto, H.: Chemistry of OH and HO_2 radicals observed at Rishiri Island, Japan, in September 2003: missing daytime sink of HO_2 and positive nighttime correlations with monoterpenes, J. Geophys. Res.-Atmos., 112, D11308, doi:10.1029/2006jd007987, 2007.

Kopacz, M., Jacob, D. J., Fisher, J. A., Logan, J. A., Zhang, L., Megretskaia, I. A., Yantosca, R. M., Singh, K., Henze, D. K., Burrows, J. P., Buchwitz, M., Khlystova, I., McMillan, W. W., Gille, J. C., Edwards, D. P., Eldering, A., Thouret, V., and Nedelec, P.: Global estimates of CO sources with high resolution by adjoint inversion of multiple satellite datasets (MOPITT, AIRS, SCIAMACHY, TES), Atmos. Chem. Phys., 10, 855–876, doi:10.5194/acp-10-855-2010, 2010.

Krol, M. and Lelieveld, J.: Can the variability in tropospheric OH be deduced from measurements of 1,1,1-trichloroethane (methyl chloroform)?, J. Geophys. Res., 108, 4125, doi:10.1029/2002jd002423, 2003.

Loukhovitskaya, E., Bedjanian, Y., Morozov, I., and Le Bras, G.: Laboratory study of the interaction of HO_2 radicals with the NaCl, NaBr, $MgCl_2$ center dot $6H_2O$ and sea salt surfaces, Phys. Chem. Chem. Phys., 11, 7896–7905, doi:10.1039/b906300e, 2009.

Macintyre, H. L. and Evans, M. J.: Parameterisation and impact of aerosol uptake of HO_2 on a global tropospheric model, Atmos. Chem. Phys., 11, 10965–10974, doi:10.5194/acp-11-10965-2011, 2011.

Mao, J., Jacob, D. J., Evans, M. J., Olson, J. R., Ren, X., Brune, W. H., Clair, J. M. St., Crounse, J. D., Spencer, K. M., Beaver, M. R., Wennberg, P. O., Cubison, M. J., Jimenez, J. L., Fried, A., Weibring, P., Walega, J. G., Hall, S. R., Weinheimer, A. J., Cohen, R. C., Chen, G., Crawford, J. H., McNaughton, C., Clarke, A. D., Jaeglé, L., Fisher, J. A., Yantosca, R. M., Le Sager, P., and Carouge, C.: Chemistry of hydrogen oxide radicals (HO_x) in the Arctic troposphere in spring, Atmos. Chem. Phys., 10, 5823–5838, doi:10.5194/acp-10-5823-2010, 2010.

Martin, R. V., Jacob, D. J., Yantosca, R. M., Chin, M., and Ginoux, P.: Global and regional decreases in tropospheric oxidants from photochemical effects of aerosols, J. Geophys. Res.-Atmos., 108, 4097, doi:10.1029/2002jd002622, 2003.

Matthew, B. M., George, I., and Anastasio, C.: Hydroperoxyl radical (HO_2) oxidizes dibromide radical anion ($^{\cdot}Br_2^-$) to bromine (Br_2) in aqueous solution: implications for the formation of Br_2 in the marine boundary layer, Geophys. Res. Lett., 30, 2297, doi:10.1029/2003gl018572, 2003.

Meinshausen, M., Smith, S., Calvin, K., Daniel, J., Kainuma, M., Lamarque, J. F., Matsumoto, K., Montzka, S., Raper, S., Riahi, K., Thomson, A., Velders, G., and van Vuuren, D. P.: The RCP greenhouse gas concentrations and their extensions from 1765 to 2300, Clim. Change, 109, 213–241, doi:10.1007/s10584-011-0156-z, 2011.

Miller, C. E. and Francisco, J. S.: The formation of a surprisingly stable HO_2-H_2SO_4 complex, J. Am. Chem. Soc., 123, 10387–10388, 2001.

Mozurkewich, M., McMurry, P. H., Gupta, A., and Calvert, J. G.: Mass accommodation coefficient for HO_2 radicals on aqueous particles, J. Geophys. Res.-Atmos., 92, 4163–4170, 1987.

Olson, J. R., Crawford, J. H., Brune, W., Mao, J., Ren, X., Fried, A., Anderson, B., Apel, E., Beaver, M., Blake, D., Chen, G., Crounse, J., Dibb, J., Diskin, G., Hall, S. R., Huey, L. G.,

Rast, S., Rodriguez, J. M., Sanderson, M. G., Savage, N. H., Strahan, S. E., Sudo, K., Szopa, S., Unger, N., van Noije, T. P. C., and Zeng, G.: Multimodel simulations of carbon monoxide: comparison with observations and projected near-future changes, J. Geophys. Res.-Atmos., 111, D19306, doi:10.1029/2006jd007100, 2006.

Sommariva, R., Haggerstone, A.-L., Carpenter, L. J., Carslaw, N., Creasey, D. J., Heard, D. E., Lee, J. D., Lewis, A. C., Pilling, M. J., and Zádor, J.: OH and HO_2 chemistry in clean marine air during SOAPEX-2, Atmos. Chem. Phys., 4, 839–856, doi:10.5194/acp-4-839-2004, 2004.

Sommariva, R., Bloss, W. J., Brough, N., Carslaw, N., Flynn, M., Haggerstone, A.-L., Heard, D. E., Hopkins, J. R., Lee, J. D., Lewis, A. C., McFiggans, G., Monks, P. S., Penkett, S. A., Pilling, M. J., Plane, J. M. C., Read, K. A., Saiz-Lopez, A., Rickard, A. R., and Williams, P. I.: OH and HO_2 chemistry during NAMBLEX: roles of oxygenates, halogen oxides and heterogeneous uptake, Atmos. Chem. Phys., 6, 1135–1153, doi:10.5194/acp-6-1135-2006, 2006.

Taketani, F., Kanaya, Y., and Akimoto, H.: Kinetics of heterogeneous reactions of HO_2 radical at ambient concentration levels with $(NH_4)_2SO_4$ and NaCl aerosol particles, J. Phys. Chem. A, 112, 2370–2377, doi:10.1021/jp0769936, 2008.

Taketani, F., Kanaya, Y., and Akimoto, H.: Heterogeneous loss of HO_2 by KCl, synthetic sea salt, and natural seawater aerosol particles, Atmos. Environ., 43, 1660–1665, doi:10.1016/j.atmosenv.2008.12.010, 2009.

Taketani, F., Kanaya, Y., and Akimoto, H.: Kinetics of HO_2 uptake in levoglucosan and polystyrene latex particles, J. Phys. Chem. Lett., 1, 1701–1704, doi:10.1021/jz100478s, 2010.

Thornton, J. and Abbatt, J. P. D.: Measurements of HO_2 uptake to aqueous aerosol: mass accommodation coefficients and net reactive loss, J. Geophys. Res.-Atmos., 110, D08309, doi:10.1029/2004jd005402, 2005.

Thornton, J. A., Jaeglé, L., and McNeill, V. F.: Assessing known pathways for HO_2 loss in aqueous atmospheric aerosols: regional and global impacts on tropospheric oxidants, J. Geophys. Res.-Atmos., 113, D05303, doi:10.1029/2007jd009236, 2008.

van Donkelaar, A., Martin, R. V., Brauer, M., Kahn, R., Levy, R., Verduzco, C., and Villeneuve, P. J.: Global estimates of ambient fine particulate matter concentrations from satellite-based aerosol optical depth: development and application, Environ. Health Perspect., 118, 847–855, doi:10.1289/ehp.0901623, 2010.

27069

Wang, Y., McElroy, M. B., Munger, J. W., Hao, J., Ma, H., Nielsen, C. P., and Chen, Y.: Variations of O_3 and CO in summertime at a rural site near Beijing, Atmos. Chem. Phys., 8, 6355–6363, doi:10.5194/acp-8-6355-2008, 2008.

27070

Table 1. Field evidence on HO_2 aerosol uptake.

Location	Type	HO_2 Conc (pptv)[a]	Estimated $\gamma(HO_2)$	Comments	Reference
Mauna Loa	remote	~ 15[b]	0.5–1		Cantrell et al. (1996)
Southern Ontario, Canada	rural	~ 10	~ 1	To reduce HO_x by more than a factor of 2	Plummer et al. (1996)
Oki Island, Japan	remote	~ 10	~ 1	To reduce HO_2 by 50 %	Kanaya et al. (2000)
TRACE-P aircraft campaign	polluted troposphere		N/A	30–50 % loss of peroxy radicals onto aerosols	Cantrell et al. (2003a)
TOPSE aircraft campaign	remote	~ 5	N/A		Cantrell et al. (2003b)
Remote marine boundary layer near Australia	remote	~ 8	1		Sommariva et al. (2004); Haggerstone et al. (2005)
Saharan dust plume	plume	~ 15[b]	1	No H_2O_2 formed from HO_2 uptake. Also needs uptake for H_2O_2	de Reus et al. (2005)
Mace Head, Ireland	remote	~ 6	1		Sommariva et al. (2006)
Rishiri Island, Japan	remote	~ 6	1		Kanaya et al. (2007)
Jungfraujoch research station[c]	remote	~ 6	1		Parker et al. (2009)
Biomass burning plumes in West Africa	plume		N/A	Modeled HO_2 is higher than measured HO_2 by a factor of 5	Commane et al. (2010)
Arctic spring	remote	~ 5	~ 1		Mao et al. (2010); Olson et al. (2012)
Arctic summer	remote	~ 10	~ 1		Olson et al. (2012)

[a] Noontime mean or median value.
[b] Estimated from the measured total peroxy radicals ($HO_2 + RO_2$).
[c] Estimated for the uptake on snow surface.
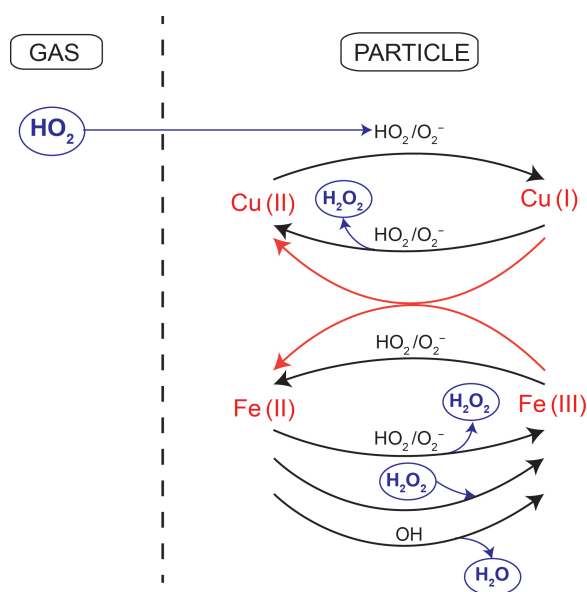
Fig. 1. Cu-Fe redox coupling in aqueous aerosols driven by HO_2 uptake from the gas phase. In the presence of dissolved Cu alone, HO_2 is converted to H_2O_2. In the presence of both dissolved Cu and Fe, HO_2 is converted to either H_2O_2 or H_2O and may also catalytically consume H_2O_2.
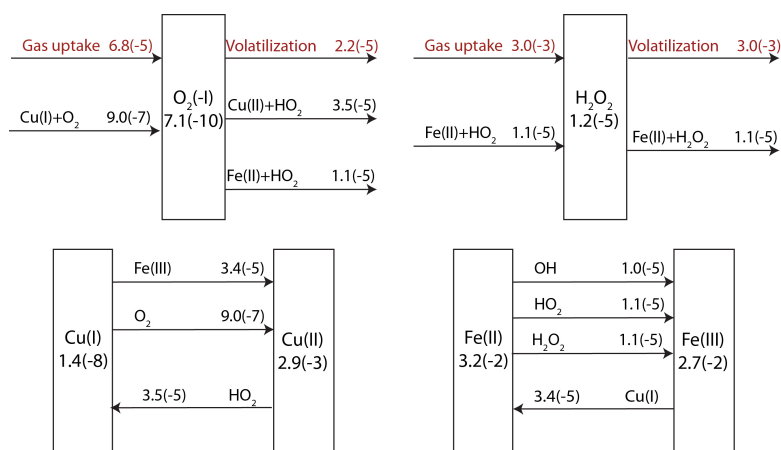
Fig. 2. Simulated aerosol budgets of $O_2(-I) \equiv HO_2(aq) + O_2^-$, H_2O_2, dissolved Cu, and dissolved Fe. The main reaction pathways are indicated. The values shown are aqueous concentrations (M) and transformation rates ($M s^{-1}$). Read 6.8(−5) as 6.8×10^{-5}. The Cu(I) + HO_2 Reaction (RA2) is not shown as it is negligibly small under these conditions. Model calculations assume an aqueous NH_4HSO_4 aerosol with dry radius of 0.35 μm at RH = 85% and T = 298 K. This simulation is constrained with $HO_2(g)$ = 10 pptv, $H_2O_2(g)$ = 1 ppb, $O_3(g)$ = 30 ppb. Aerosol pH is 0.15 with ionic strength 7.8 mol kg^{-1} (the resulting activity coefficient $A(Cu^{2+})$ = 0.067). Dissolved Cu concentration is 2.9×10^{-3} M, adopted from Ross and Noone (1991). The dissolved Cu to Fe ratio is Cu/Fe = 0.05.
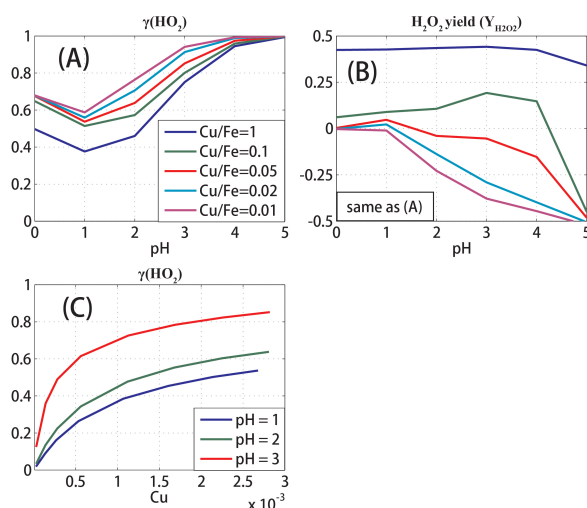
Fig. 3. Impacts of Cu-Fe-HO$_x$ cycling on aerosol chemistry for the model calculations described in the text. **(A, B)** pH dependence of the HO_2 reactive uptake probability $\gamma(HO_2)$ and the corresponding H_2O_2 yield for different Cu/Fe molar ratios. **(C)** Dependence of $\gamma(HO_2)$ on Cu concentrations for different pH values with Cu/Fe = 0.05.

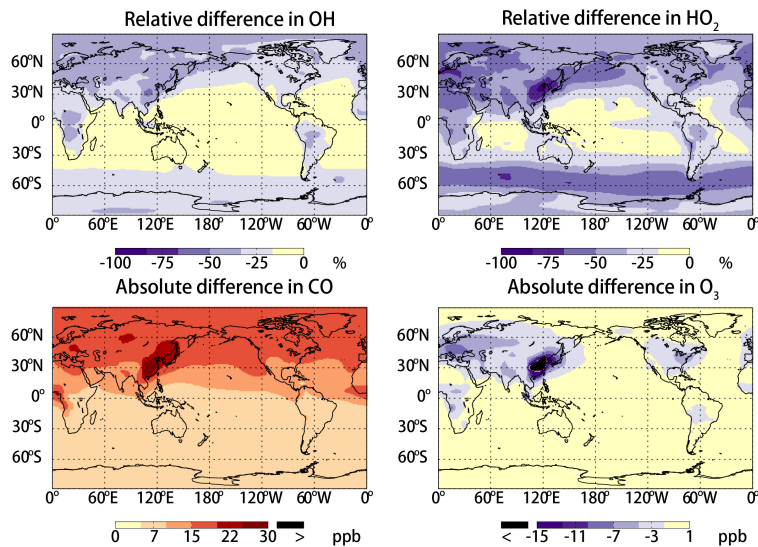**Fig. 4.** Effect of HO$_2$ reactive uptake on non-cloud aerosols (γ(HO$_2$) = 1 producing H$_2$O) on surface air concentrations of OH, HO$_2$, CO, and O$_3$ in the GEOS-Chem model. Values are annual means for 2005 and are calculated by difference with a simulation including no HO$_2$ uptake.
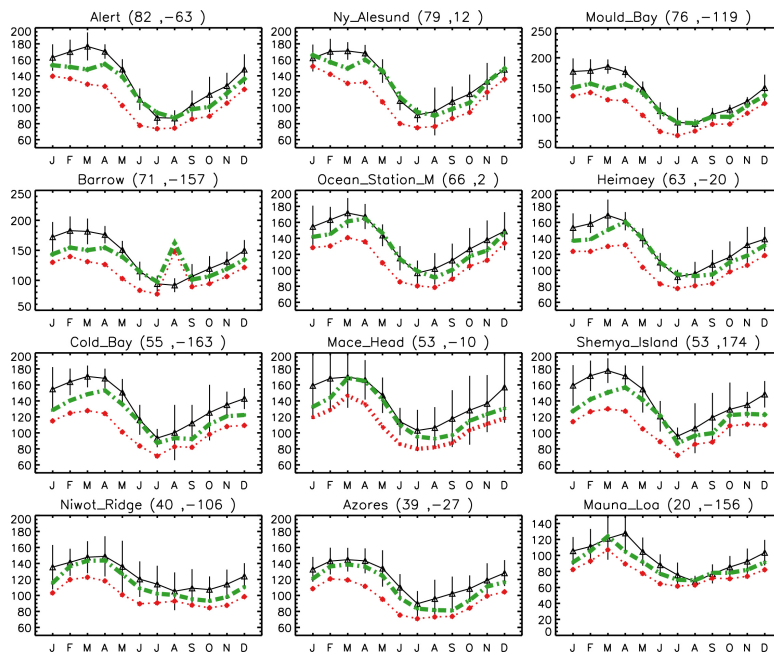
Fig. 5. Seasonal variation of CO concentrations at remote surface sites in northern extratropics. Climatological observations from NOAA/GMD (1988–2007) are shown in black. GEOS-Chem model values are shown in red with no HO$_2$ uptake and in green with γ(HO$_2$) = 1 producing H$_2$O.